Resonance Raman Microspectroscopic Characterization of Eosinophil Peroxidase in Human Eosinophilic Granulocytes

B. L. N. Salmaso,* G. J. Puppels,* P. J. Caspers,* R. Floris,‡ R. Wever,‡ and J. Greve*

*Department of Applied Physics, University of Twente, 7500 AE Enschede, and ‡E. C. Slater Institute, University of Amsterdam, Plantage Muidergracht 12, 1018 TV Amsterdam, The Netherlands

ABSTRACT   A resonance Raman microspectroscopic study is presented of eosinophil peroxidase (EPO) in human eosinophilic granulocytes. Experiments were carried out at the single cell level with laser excitation in Soret-, Q_v-, and charge transfer absorption bands of the active site heme of the enzyme. The Raman signal obtained from the cells was almost exclusively due to EPO. Methods were developed to determine depolarization ratios and excitation profiles of Raman bands of EPO in situ. A number of Raman band assignments based on earlier experiments with isolated EPO have been revised. The results show that in agreement with literature on isolated eosinophil peroxidase, the prosthetic group of the enzyme in the (unactivated) cells is a high spin, 6-coordinated, ferric protoporphyrin IX. The core size of the heme is about 2.04 Å. The proximal and distal axial ligands are most likely a histidine with the strong imidazolate character typical for peroxidases, and a weakly bound water molecule, respectively. The data furthermore indicate that the central iron is displaced from the plane of the heme ring. The unusual low wavenumber Raman spectrum of EPO, strongly resembling that of lactoperoxidase, intestinal peroxidase and myeloperoxidase, suggests that these mammalian peroxidases are closely related, and characterized by, as yet unspecified, interactions between the peripheral substituents and the protein, different from those found in other protoheme proteins.

INTRODUCTION

In humans eosinophilic granulocytes make up a small fraction (~2%) of the white blood cells, circulating in the blood. They play an important, but still not well characterized, role in the nonspecific immunologic defense of the body against parasites and are negative modulators in immunoinflammation (Parker, 1984; Butterfield et al., 1984). Recently, it was found that an eosinophil-dependent mechanism exists for the tumor cytotoxic effect of interleukin-4 (Tepper et al., 1992). In the cytoplasm of eosinophils, approximately 200 granules are present, with an average diameter of 0.9–1.3 μm (Klebanoff and Clark, 1978). Electron microscopy has shown that these granules consist of an electron-dense core, surrounded by a less electron-dense matrix. The core consists of a single type of protein, called Major Basic Protein. The matrix contains a high concentration of eosinophil peroxidase (EPO). On average, 15 pg of EPO per cell is found (Butterfield et al., 1984; Gleich and Adophson, 1986). The enzyme is composed of two subunits with a molecular mass of 58 and 14 kDa, respectively (Bolscher et al., 1984). The protein is highly basic and tends to aggregate. Therefore, it can only be isolated in high salt solutions or in detergents. EPO is involved in the killing process after the attachment of eosinophils to parasites or after phagocytosis, after which the granule contents are discharged onto the parasite surface. It has been proposed that the function of the enzyme is to produce cytocidal hypohalites via an EPO + H_2O_2 + halide

reaction mechanism. Just like myeloperoxidase, the peroxidase found in neutrophils and monocytes, EPO can produce hypochlorous acid in the presence of chloride and peroxide (Wever et al., 1981). But parasites are killed most effectively in the presence of bromide (Ramsey et al., 1982; Klebanoff et al., 1989). The precise mechanisms involved in EPO activation and inactivation, as well as in most other peroxidases, still have to be elucidated.

Information about the structure of the EPO prosthetic group has been obtained by EPR of whole cells (Wever et al., 1980) and absorption spectroscopy (Bolscher et al., 1984) and Raman spectroscopy of isolated EPO (Sibbett et al., 1985). The general picture that has arisen from these studies is that the chromophore in EPO is a protoporphyrin IX, which is also present in other peroxidases such as horseradish peroxidase (Kitagawa et al., 1986, Terner et al., 1984) and lactoperoxidase (Kitagawa et al, 1983), and in hemoglobin (Spiro, 1983). The resting enzyme is thought to possess a 6-coordinated high spin ferric heme group.

The important advantage of resonance Raman spectroscopy over other spectroscopic techniques is that it can be applied to study the structure of the heme of the enzyme in situ at the level of a single living cell so that ultimately it may be possible to directly link changes in this structure to processes taking place in the cell. It is necessary, therefore, to determine which information about EPO in the cell can be obtained from Raman studies and under which conditions. Earlier we reported that, when measuring in the cytoplasm of granulocytes, strong Raman signal contributions can be obtained of myeloperoxidase in the case of neutrophils and of EPO in the case of eosinophils (Puppels et al., 1991b). In this paper, we show that EPO can be characterized intracellularly by means of Raman spectroscopy and make clear which information can be obtained about its prosthetic group,

using laser excitation in the Soret-, Q_v-, and Charge Transfer-absorption bands. The new data obtained extend the Raman spectroscopic study of isolated EPO of Sibbett et al. (1985) to the wavenumber region below 900 cm^{-1} and also make it necessary to reconsider the assignments of the Raman bands of EPO made in that paper. The techniques and methods used here should be readily applicable to the in situ structural characterization of other heme-compounds.

MATERIALS AND METHODS

Sample preparations

For all measurements shown (Raman and absorption spectroscopy), peripheral blood eosinophils were used, isolated according to the method of Koenderman et al. (1988). Fresh buffycoats of human blood were obtained from the local Central Blood bank (Enschede).

For the absorption spectroscopic measurement, a sample of human eosinophilic granulocytes of a purity >99% was donated by Drs. T. Kuijpers and A. Tool of the department of Blood cell Chemistry of the Netherlands Red Cross Central Laboratory in Amsterdam. The final concentration of the cell suspension used in the experiments was 2×10^7 cells/ml.

Native (oxidized) human EPO was isolated from outdated buffycoats following the procedure of Wever et al. (1981). The absorption ratio $A_{412\,nm}/A_{280\,nm}$ of the EPO sample was 0.2. The sample was stored at $-20°C$ until the measurements, which were carried out at room temperature.

Human myeloperoxidase was isolated according to the method described in Bakkenist et al. (1978).

Bovine lactoperoxidase was purchased from Sigma Chemical Co. (St. Louis, MO) and was used without further purification.

Raman instrumentation and measurements

Raman spectra of eosinophils and of isolated EPO were measured using the confocal Raman microspectrometer described in detail by Puppels et al. (1990, 1991a). To enable recording of spectra using laser wavelengths other than 660 nm, for which the set-up was originally designed, the recording was slightly modified. For the experiments with 514.5 nm laser excitation (from a Coherent Innova 90 Argon-ion laser), a narrow bandpass filter was used to couple microscope and spectrometer. A holographic edge filter (Physical Optics Corp., Torrance, CA) was used to suppress the intensity of the scattered laser light entering the spectrometer. For the experiments carried out to determine excitation profiles of Raman lines between 623 and 676 nm (from a Spectra-Physics 375B dye laser, operated with DCM and pumped by the Argon-ion laser mentioned above), a semitransparent mirror was used for coupling of microscope and spectrometer. One or two holographic notch filters (Kaiser Optical Systems, Inc., Ann Arbor, MI), which were angle-tuned to the laser wavelength, were used to suppress laser light. Experiments with 413.1-nm excitation (Coherent Innova 90-K Krypton-laser) were performed on a different, newly built instrument. The most important difference with the set-up mentioned above is that it is equipped with a liquid nitrogen-cooled CCD-camera fitted with a Tektronix 512TKB thinned back-illuminated CCD-chip, which shows a very good response in the blue spectral region (quantum efficiency at 400 nm > 60% (Princeton Instruments, Inc., Trenton, NJ). Also, in this case laser line suppression was achieved with a holographic notch filter (Kaiser Optical Systems).

For the experiments with cells a x63 Zeiss Plan Neofluar water immersion objective (numerical aperture 1.2) was used to focus laser light on the sample and to collect scattered light. In this configuration, the spatial resolution of the CRM is $\sim 0.45 \times 0.45 \times 1.3 \,\mu m^3$ (Puppels et al., 1991a).

Eosinophils were deposited on a fused silica substrate, coated with poly-L-lysine, and immersed in Hank's buffered salt solution (prepared according to Gibco HBSS nr. 041–04025, phenol red omitted; Gibco BRL Life Technologies, Breda, The Netherlands). The cells typically have a diameter of 12–15 μm. Due to the many dense granules, cytoplasm and nucleus are easily distinguishable. The spectra shown, therefore, are free of signal contributions from the nucleus of the eosinophils. They are averages of 20–40 measurements on different cells, using ~ 6 mW (for excitation between 623 and 676 nm), 3 mW (excitation at 514.5 nm), or 0.5 mW (excitation at 413.1 nm) of laser power on the sample and a signal integration time of 30 s per measurement (except for the measurements with 413.1-nm excitation, where a signal integration time of 10 s was used). Under these conditions no laser-induced spectral changes were observed. Two consecutive measurements on the same position in the cell yielded identical spectra. Only with 413.1-nm excitation some bleaching of Raman signal occurred ($\sim 30\%$ lower signal intensity in the second measurement) without changes in line positions or line shapes however.

The measurements on the isolated EPO were carried out with the sample at a concentration of about 100 μM in a 200 mM potassium phosphate solution (pH 7.2) with 0.5% of Tween 80, contained in square capillary glass tubes (inner dimension 500 μm, wall thickness 100 μm; Vitro Dynamics Inc, Rockaway, NJ), using a 63$\times$ Zeiss Plan Neofluar water immersion objective with cover glass correction. A laser power of 15 mW was used (660 nm). The spectra are the result of an average of 10 measurements of 300 s integration time each. The measurements on isolated myeloperoxidase (40 μM in 100 mM phosphate buffer, pH 7.2) and lactoperoxidase (77 μM in 100 mM phosphate buffer, pH 7.2) were carried out in the same way, using ~ 400 μW of laser power at the sample (413.1 nm).

A Spindler & Hoyer 10K polarizer was used to analyze the polarization characteristics of the Raman scattered light. Depolarization effects due to the use of a high numerical aperture microscope objective (Turrell, 1984; Bremard, 1985) were limited to 1–2%, which followed from tests in which the depolarization ratio of chloroform lines was measured. No corrections were made, because such small effects were not important for the interpretation of the data. All measurements were carried out at room temperature.

The Raman spectra shown were processed by means of the software package RAMPAC (De Mul and Greve, 1993). An indene spectrum, recorded with the same instrument setting as used in the measurements was used for the wavenumber calibration of the spectra. By this procedure, variations in peak positions between different experiments are limited to 2 cm^{-1}. The spectra have been corrected for the wavelength- and polarization-dependent signal detection efficiencies of the instruments used and for pixel-to-pixel variations in CCD-detector sensitivity (Puppels et al., 1991a). Buffer signal contributions have been subtracted. In the Raman spectra from the cells, signal-to-background ratios were >1:2 for all laser excitation wavelengths employed. Autofluorescence of eosinophils, therefore, did not constitute any problem in our measurements.

Determination of depolarization ratios and excitation profiles of EPO in situ

Cells are inhomogeneous, which makes the determination of depolarization ratios and excitation profiles less straightforward than in the case of a homogeneous sample. The intensity of the Raman signal depends linearly on the number of molecules in the measuring volume and, therefore, shows considerable variations from one cell measurement to the next. All spectra shown are averaged over 20 or more measurements on different cells, which partly corrects for this. However, an *intrinsic normalization* of signal intensities is needed, to avoid sample inhomogeneity affecting the results.

To determine the depolarization ratio of the EPO Raman bands in cells, measurements were carried out in the absence of a polarizer (unpolarized) and in the presence of a polarizer (polarized and depolarized). The unpolarized spectrum was subsequently fitted with the polarized and depolarized spectra. The EPO spectra, obtained with 660- and 514.5-nm excitation, were found to contain polarized, depolarized, and anomalously polarized bands, which makes such a procedure possible. The fit-factors thus found have a margin of error of 5% (660 nm) and 7% (514.5 nm). These margins are representative of the variations in fit-factors for different lines in the Raman spectra. The intensities of the Raman bands in the polarized and depolarized spectra multiplied by the factors needed to obtain a good fit of the unpolarized spectrum were used to determine the depolarization ratios. This was done by subtracting the polarized from the depolarized spectrum (both multiplied by the fit factors) in such a way that the Raman band under investigation disappeared in the difference spectrum. The factor by which

FIGURE 1   Absorption spectrum of a suspension of human eosinophilic granulocytes (2×10^7 cells/ml).
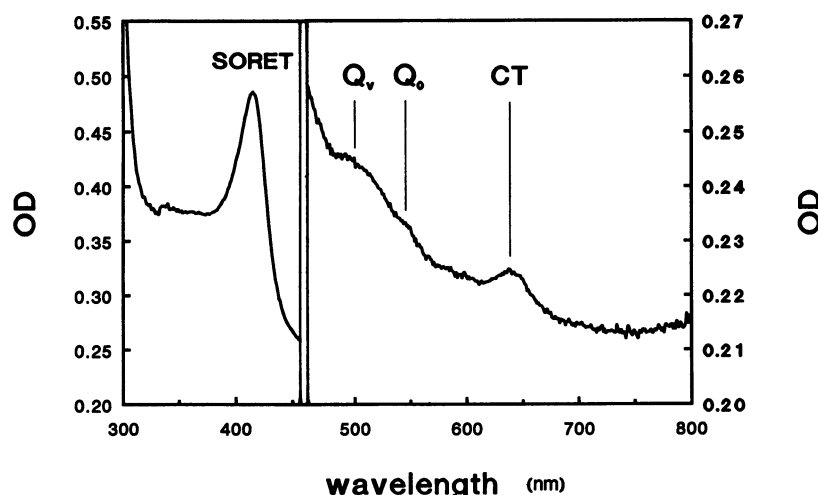
the polarized spectrum had to be multiplied to achieve this is the depolarization ratio given in Table 1. The depolarization ratios thus determined are accurate to about 10% for strong, well separated lines and to about 20% for weaker lines. This sufficed to categorize lines as polarized, depolarized, or anomalously polarized, which was the information needed to assign Raman lines to specific vibrational modes. Multiple light scattering events, which occur in eosinophils, due to the many dense cytoplasmic granules, can lead to depolarization of the scattered light. In flowcytometric experiments, depolarization in the order of a few percent of the elastically scattered light was observed (De Grooth et al., 1987). To check whether multiple scattering events would affect noticeably the depolarization ratios determined for EPO in situ, they were compared with those found for isolated EPO (using 660-nm excitation). For all lines, the depolarization ratios for isolated EPO and EPO in situ were found to corresponded within the margins of error mentioned above. All of the strong EPO lines in the eosinophil spectra obtained with 413.1-nm excitation had the same relative intensity in polarized and depolarized spectra. Therefore, the fit-procedure described above could not be applied to obtain their precise depolarization ratio. The figures mentioned in Table 1 were taken from the work on isolated EPO of Sibbett et al. (1985).

Also, for the determination of excitation profiles in the wavelength region from 623 to 676 nm, an intrinsic normalization procedure was needed to avoid effects of sample inhomogeneity. Therefore, all spectra were normalized with respect to the 1004 cm^{-1} phenylalanine band, which is prominently present in the spectra obtained with red laser light excitation. This line was chosen because it is always present in cell spectra in an almost fixed intensity ratio ($\pm10\%$) to Raman bands originating from the EPO heme-ring. This 10% variation in relative phenylalanine Raman band intensity does not affect the results, because for each point of the excitation profile 20 single cell spectra were averaged. (Normalization on the 1448-cm^{-1} band, which is primarily due to protein CH_2/CH_3 bending modes, resulted in virtually the same scaling factors.) Then the intensities of the Raman bands in the normalized spectra obtained with different laser excitation wavelengths were determined relatively to the intensity of the corresponding bands in the spectrum obtained with 638-nm excitation (which together with 646 nm excitation resulted in the highest signal intensities). For this, the same difference-spectrum procedure was used as for the determination of depolarization ratios described above. In Fig. 4, the excitation profiles thus obtained are shown.

Absorption spectroscopy

Human eosinophilic granulocytes are very strong light scatterers (De Grooth et al., 1987). Therefore, the absorption measurements on eosinophil suspensions were carried out on a spectrophotometer (Perkin-Elmer 551S) equipped with an Ulbricht 45°-integrating sphere, to minimize intensity losses due to light scattering. From the measured spectrum a first-order polynome was subtracted to correct for residual light scattering losses and for clarity of presentation.

RESULTS

Fig. 1 shows an absorption spectrum of a suspension of eosinophils. It is identical to that of the isolated native (oxidized) EPO (Bolscher et al., 1984), indicating that this enzyme is mainly responsible for the absorption of the cells in the wavelength region shown. It resembles absorption spectra of Fe^{3+} high spin heme compounds such as ferrimyoglobin (Eaton and Hochstrasser, 1968), native lactoperoxidase (Manthey et al., 1986), and native intestinal peroxidase (Kimura et al., 1981). The absorption bands have been assigned in agreement with Eaton and Hochstrasser (1968). The spectrum shows the typical strong Soret band at 412 nm. A number of weak bands are visible at higher wavelengths. The Q_v and Q_0 π-to-π^1 transition bands are very weak (maxima at 500 and 550 nm, respectively). A stronger absorption band, due to the π-to-d_π charge transfer (CT) transition, is found at 640 nm.

Raman experiments were carried out, focusing laser light to a nearto diffraction-limited spot in the cytoplasmic region

---

[1] In earlier work on lactoperoxidase and intestinal peroxidase (Kitagawa et al., 1983; Kimura et al., 1981), a different assignment for the ν_2 vibration was proposed (at 1593 cm^{-1} in lactoperoxidase and at 1586 cm^{-1} in intestinal peroxidase) based on experiments using laser excitation at 441.6 nm, i.e., $\sim$30 nm from the Soret band maximum. Although the spectra in those papers are very similar to those of Manthey et al. (1986) and those of EPO (this work and Sibbett et al. 1985) obtained under excitation at the Soret maximum, the depolarization ratios that were reported for the high frequency bands are different, most likely because of the difference in excitation wavelength. The apparent excitation of depolarized and anomalously polarized lines upon excitation at 441.6 nm makes the correct assignment of the ν_2 vibration (A_{1g}, polarized) based on band depolarization ratios difficult, because its spectral position is often very close and strongly overlapping with those of the ν_{19} (A_{2g}, anomalously polarized and enhanced under Q_v-excitation) and ν_{11} (B_{1g}, depolarized), resulting in an erroneous assignment of ν_2 to the ν_{37} mode (Kitagawa et al. 1983; Kimura et al., 1981).
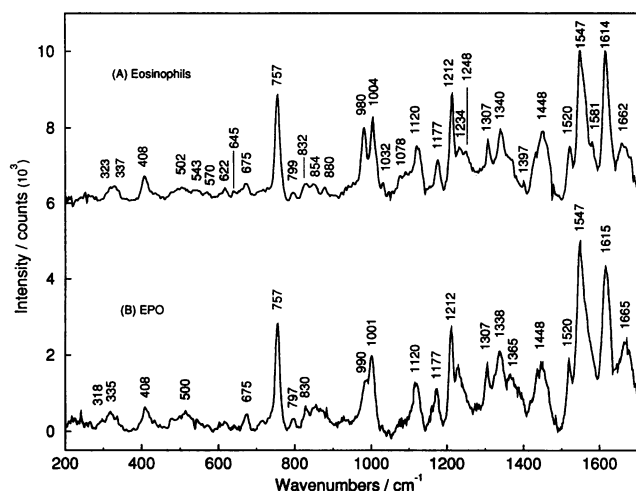
FIGURE 2 Raman spectra obtained with 660 nm laser excitation. (A) Eosinophil cytoplasmic granules, average of 20 measurements on different cells. Laser power on sample 6 mW. Signal integration time 30 s/measurement. (B) 100 μM sample of isolated native (oxidized) human EPO in a 200 mM potassium phosphate solution (pH 7.2) and 0.5% Tween 80. Laser power on sample 15 mW. Signal integration time 300 s/measurement. Average of 10 measurements. For both spectra, the high and low wavenumber regions were measured separately. The resulting spectra were joined at 900 cm⁻¹ after normalization on the 757-cm⁻¹ band. Spectrum B was scaled to have equal intensity in the 757-cm⁻¹ band as for the cell spectrum. For clarity of presentation, spectrum A was shifted along the ordinate and for both spectra a slightly sloping background was corrected for by subtraction of a first-order polynome.
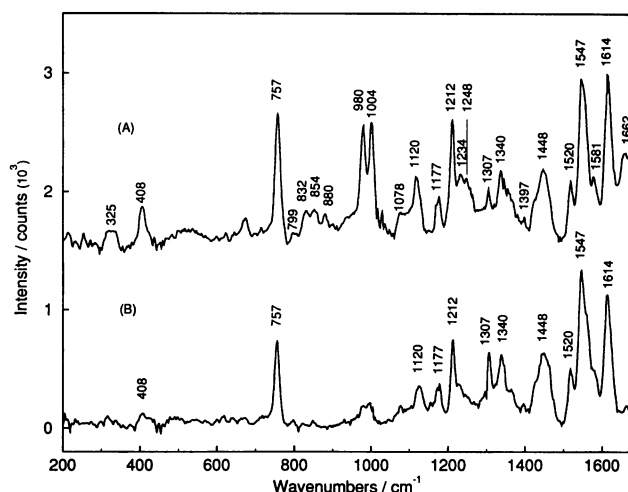

FIGURE 3 Polarized (A) and depolarized (B) Raman spectra obtained from the eosinophil cytoplasmic region with excitation in CT-absorption band, using 660 nm laser light. Laser power on sample 7 mW. Spectra were averaged over 30 (spectrum A) and 40 (spectrum B) measurements on different cells. Signal integration time: 30 s/measurement. Background subtraction and joining of high and low cm⁻¹ regions; see caption of Fig. 2. Spectra were scaled by the factors needed to fit the unpolarized spectrum; the method is described in Materials and Methods. Spectrum A is shifted along ordinate for clarity of presentation.

of human eosinophils, with laser excitation in the CT absorption band of EPO, with laser excitation at 514.5 nm in the Q_v-absorption band and with laser excitation in the Soret band at 413.1 nm.

A comparison of the spectrum of eosinophils with that of the isolated enzyme (Fig. 2) makes clear that the Raman signal obtained from eosinophils upon excitation at 660 nm in the CT band is almost exclusively due to EPO. A noticeable difference is the absence of the line at 980 cm⁻¹ in the spectrum of the isolated EPO. Because this line is always present in the eosinophil spectra and with a constant intensity relative to the EPO-lines, it must be due to an as yet unidentified compound, present in the cytoplasmic granules, that contains the EPO.

The polarized and depolarized Raman spectra of eosinophils, obtained with 660 nm laser excitation (Fig. 3), show the presence of polarized, depolarized, and anomalously polarized Raman lines (Table 1 gives line-assignments and depolarization ratios, calculated according to the procedure given in Materials and Methods).

Fig. 4 shows excitation profiles of a number of Raman bands of the enzyme in the wavelength interval from 623 to 676 nm, measured in situ. It illustrates the resonance enhancement of Raman signal upon excitation in the CT-absorption band and the fact that different enhancement mechanisms are involved for Raman bands assignable to vibrational modes of different parts of the heme-group. The results resemble those of Asher et al. (1977), obtained for methemoglobin fluoride, a ferric high spin heme compound.
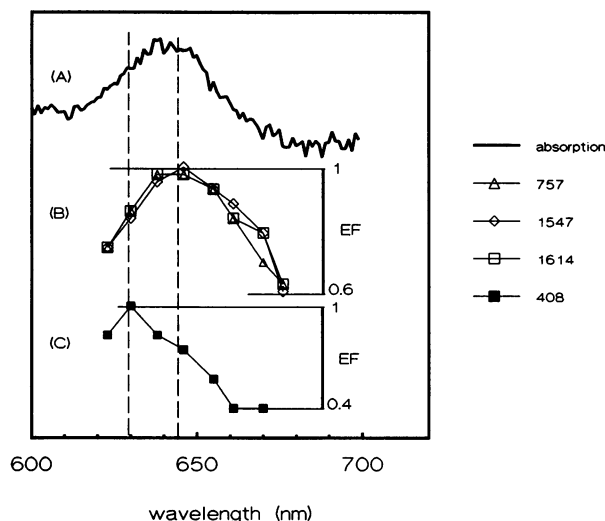

FIGURE 4 Excitation profiles of Raman bands of EPO measured in cells. (A) CT absorption band of EPO in eosinophils (detail of Fig. 1). (B) Excitation profiles of the ν_{10} (1614 cm⁻¹), ν_{11} (1547 cm⁻¹), and ν_{16} (757 cm⁻¹) EPO Raman bands. (C) Excitation profile of the 408 cm⁻¹ EPO Raman band. EF: enhancement factor.

In Fig. 5 the unpolarized, polarized, and depolarized Raman spectra of eosinophils obtained with excitation at 514.5 nm in the Q_v absorption band are shown. In contrast with the Soret (Fig. 6) and CT (Figs. 2 and 3) spectra, low wavenumber vibrations (<700 cm⁻¹) were not observed here. The oxidation state marker band ν_4 (1369 cm⁻¹), which is not visible with excitation at 660 nm, and a band at 1558 cm⁻¹ that is only visible as a shoulder upon excitation at 660 nm
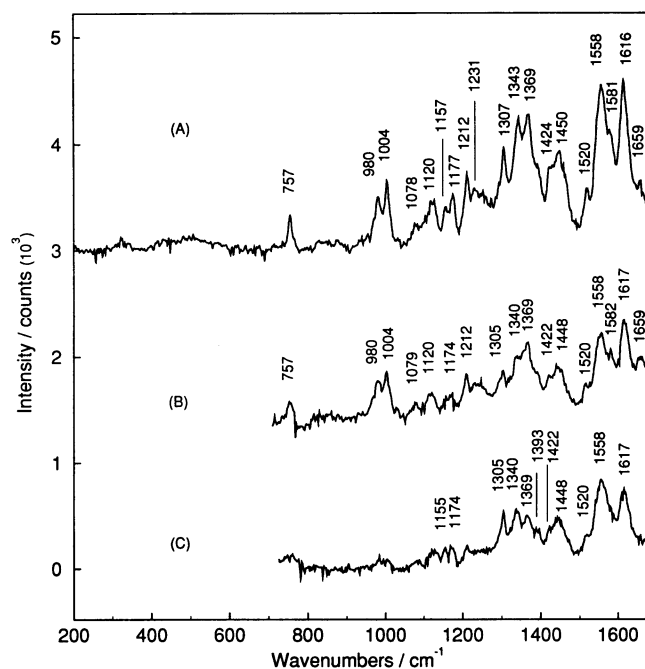
FIGURE 5   Unpolarized (A), polarized (B), and depolarized (C) Raman spectra obtained from eosinophil cytoplasmic granules with 514.5 nm laser excitation in Q_v-absorption band. Laser power on sample 4 mW. Spectra averaged over 20 measurements on different cells (low wavenumber region of spectrum A averaged over 40 measurements. Joining of low and high wavenumber spectral regions is described in caption of Fig. 2). Signal integration time 30 s/measurement. Spectra B and C were scaled by the factors needed to fit the unpolarized spectrum (A). Spectra A and B are shifted along ordinate for clarity of presentation.
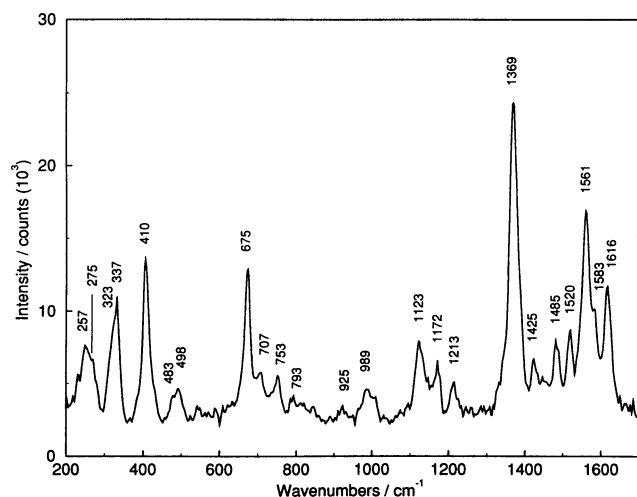

FIGURE 6   Raman spectrum obtained from eosinophil cytoplasmic granules with laser excitation in Soret absorption band (413.1 nm). Laser power on sample 0.4 mW. Spectra averaged over 10 measurements on different cells. Signal integration time 10 s/measurement.

show up clearly in these spectra. Fig. 6 shows the Raman spectrum obtained from eosinophils with laser excitation at 413.1 nm in the Soret band. The intensity of lines in the low wavenumber region (<700 cm^{-1}), where among others vibrational modes involving the central iron and the axial li-
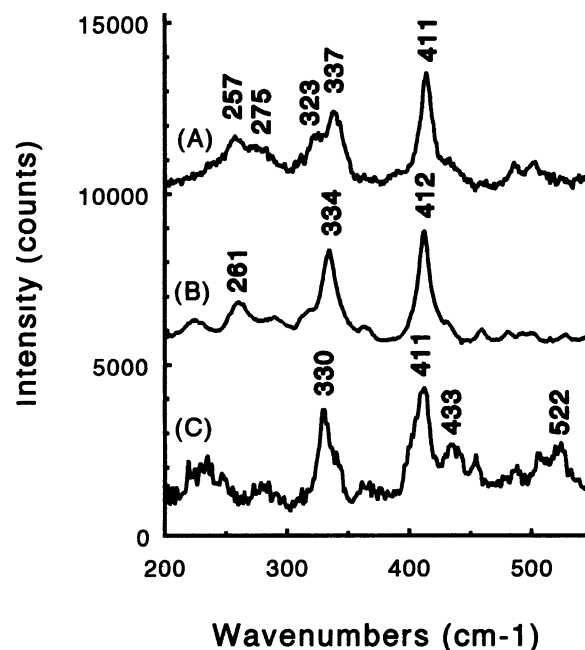

FIGURE 7   Low wavenumber Raman spectra of peroxidases at $\sim$1-cm^{-1} resolution. (laser excitation 413.1 nm). (A) EPO in situ (eosinophilic cytoplasmic granules). (B) 77 μM Lactoperoxidase. (C) 44 μM Myeloperoxidase. Laser power on sample 0.4 mW. Spectrum A averaged over 20 measurements on different cells: signal integration time 10 s/measurement. Total signal integration time for spectra A and C was 400 s. Intensity scale for spectrum A (B and C normalized with respect to intensity of the band at 411 cm^{-1}). Spectra A and B are shifted along ordinate for clarity of presentation.

gands of the heme ring are expected, is very high. The spectrum is almost identical to that of isolated EPO, obtained with 406.7-nm excitation (Sibbett et al., 1985). However, in the high wavenumber region a number of bands are found at larger wavenumber shifts than were reported in that work. Among these is the ν_4-band, the marker band for π-electron density (strongly correlated to the iron oxidation state), which was reported to have an unusually low frequency (1365 cm^{-1}) for a Fe^{3+} protoporphyrin (Sibbett et al., 1985). It is found at 1369 cm^{-1} here, in agreement with the result obtained with 514.5-nm excitation (both in our work (Fig. 5) and that of Sibbett et al. (1985)).

Fig. 7 illustrates the great similarity of the low wavenumber Raman spectra of EPO, lactoperoxidase, and myeloperoxidase, obtained with 413.1 nm laser excitation. These spectra of mammalian peroxidases are quite different from those of other heme-proteins.

DISCUSSION

Raman and absorption spectroscopic properties (this work) as well as the EPR spectroscopic properties (Wever et al., 1980) of eosinophilic granulocytes are almost completely determined by the large amounts of EPO in the cytoplasmic granules. The results obtained here make clear that EPO can be studied in single living cells by means of Raman microspectroscopy. It proved possible to determine depolarization ratios and excitation profiles of Raman bands of the enzyme in situ.

TABLE 1　Assignment of EPO Raman bands

| λ_{exc} (nm) | | | | | | Assignment | | | | |
| 660 | | 514.5 | | 413.1 | | Porphyrin modes | | | Vinyl modes | Other |
Freq. (cm^{-1})	Depol. ratio	Freq. (cm^{-1})	Depol. ratio	Freq. (cm^{-1})	Depol. ratio*	Mode number	Symm D_{4h}	Main contribution		
1662	0.2	1659								Amide I
				1616	0.3				$\nu(C{=}C)$	
1614	0.8	1616	0.6			ν_{10}	B_{1g}	$\nu(C_aC_m)$		
1581		1581		1583	0.3	ν_{37}	E_u	$\nu(C_aC_m)$		
				1561	0.2	ν_2	A_{1g}	$\nu(C_bC_b)$		
		1558	0.8			ν_{19}	A_{2g}	$\nu^1(C_aC_m)$		
1547	0.8					ν_{11}	B_{1g}	$\nu(C_bC_b)$		
1520	0.8	1520	0.5	1520	0.2	ν_{38}	E_u	$\nu(C_bC_b)$		
				1485	0.3	ν_3	A_{1g}	$\nu(C_aC_m)$		
1448	0.8	1450	0.75							CH_2/CH_3
		1424	0.8	1425	0.7				$\delta_s(=CH_2)_{(1)}$	
		1369	0.4	1369	0.3	ν_4	A_{1g}	$\nu(C_aN)$		
1340	0.85	1343							$\delta_s(=CH_2)_{(2)}$	
1307	2	1307	1.2			ν_{21}	A_{2g}	$\delta^1(C_mH)$		
									$\delta(CH{=})$	
1234		1231				ν_{13}	B_{1g}	$\delta(C_mH)$		
1212	0.75	1212	0.4	1213	0.3	$\nu_5 + \nu_{18}$				
177?	0.6	1177?		1172	0.5	ν_{30}	B_{2g}	$\nu^1(C_bS)$		
		1157							$\nu(C_b{-}C_a)_{(1)}$	
1120	0.6	1120	0.4	1123	0.3	ν_{44}	E_u	$\nu(C_bS)$		
									$\nu(C_b{-}C_a)_{(2)}$	
1032										phenylalanine
1004		1004	0.2							phenylalanine
				989		ν_{45}	E_u	$\nu^1(C_3N)$		
980		980	0.2							
757	0.65	757	0.4			ν_{16}	B_{1g}	$\delta(C_aNC_a)$		
675	0			675		ν_7	A_{1g}	$\delta(C_bC_aN)$		
622										phenylalanine
~500				498				pyrrole fold		
				483						
408	0.25			410					$\delta(C_bC_aC_\beta)_{(1)}$	$\nu_{34} + \nu_{35}$ metal-ligand
~330				337					$\delta(C_bC_aC_\beta)_{(2)}$	
				323		ν_8	A_{1g}	$\delta(C_bS)$		
				275		ν_{52}	E_u	$\delta(C_bS)$		
253				257						$\nu(Fe\text{-}His)$

Margin of error for depolarization (depol.) ratios ± 10–20% (see Materials and Methods).

* Depolarization ratios taken from Sibbett et al. 1985.

Symmetry species are for the D_{4h} symmetry; C_a, C_b, C_m denote the a, b, and meso carbon atoms of the porphyrin ring, respectively; S: peripheral substituent in the D_{4h} symmetry; ν^1 and δ^1 denote antisymmetric stretching and deformation. For the vinyl assignment: $\delta_s(=CH_2)$, in-plane CH_2 symmetric bending; $\delta(CH{=})$, CH deformation; $\nu(C_b{=}C_a)$, ring-vinyl stretch; $(C_\beta C_a C_\beta)$, vinyl bending mode; (1) and (2) denote in-phase and out-of-phase vinyl modes.

Despite the fact that in the literature several reports have appeared describing the strong autofluorescence of eosinophils (Fuerst and Jannach, 1965; Weil and Chused, 1981; Samoszuk and Espinoza, 1987), no strong fluorescent background was observed in the Raman experiments described here, with any of the laser excitation wavelengths used. Recent work of Barnes et al. (1993) might offer an explanation for this. They found that eosinophils isolated from peripheral blood had fluorescence excitation and emission spectra different from those in tissue or bone marrow studied previously (Fuerst and Jannach, 1965; Samoszuk and Espinoza, 1987). Eosinophils from peripheral blood, which were used in the present study, were found to have fluorescence excitation maxima in the UV at 280, 360, and 380 nm, whereas eosinophils from bone marrow, cervix, and colonic mucosa also showed strong fluorescence emission (around 550 nm) upon excitation at 500 nm. Moreover, it was noted that formalin or acetic acid and ethanol-fixed cells and tissues used in previous work (Fuerst and Jannach, 1965; Weil and Chused, 1981; Samoszuk and Espinoza, 1987) showed significantly stronger autofluorescence, both with 370- and 500-nm excitation, than unfixed cells (Barnes et al., 1993). For these reasons, unfixed peripheral blood eosinophils are most suitable for a Raman spectroscopic study of EPO in situ.

Assignment of Raman bands

In Table 1 the Raman bands observed with excitation at 413.1, 514.5, and 660 nm are listed. Depolarization ratios were determined according to the procedure described in Materials and Methods. The assignment of EPO Raman bands was based on these depolarization ratios, on the observed dependence of signal intensities upon excitation wavelength, and on band assignments found in the literature

for nickel(II)-octaethyl-porphyrinato (Abe et al., 1978), nickel(II)protoporphyrin IX, protoheme complexes (Choi et al., 1982a, b; Choi and Spiro, 1983), and protoheme-containing proteins like hemoglobin (Choi et al., 1982; Spiro, 1975; Spiro and Strekas, 1974), lactoperoxidase (Kitagawa et al., 1983; Manthey et al., 1986), horseradish peroxidase (Kitagawa et al., 1986; Terner et al., 1984) cytochrome c peroxidase (Smulevich et al., 1991b), intestinal peroxidase (Kimura et al., 1981), and different catalases (Sharma et al., 1989; Chuang, 1989).

In the ideal case of a heme group with D_{4h} symmetry, resonance enhancement is expected for totally symmetric modes (polarized) with excitation in the Soret region, and for non-totally symmetric modes (depolarized, anomalously polarized) upon excitation in the Q-bands (Spiro and Li, 1983). Enhancement of both heme macrocycle and iron-ligand vibrational modes has been detected with excitation in the in-plane π-to-d_π CT-transition, of ferric high spin 6-coordinated methemoglobin fluoride, at about 600 nm (Asher et al., 1977).

In the high wavenumber region, a number of assignments differ from those proposed in the work on isolated EPO by Sibbett et al. (1985). This concerns the assignments of the bands at 1581, 1561, 1547, 1512, and 1477 cm^{-1}. The bands at 1561 and 1485 cm^{-1} (1557 and 1477 cm^{-1}, respectively, in Sibbett's work) are strongly resonance-enhanced upon excitation in the Soret band, indicating that they are due to totally symmetric modes (A_{1g} in D_{4h} symmetry). This has led us to assign these bands to ν_2 and ν_3, respectively, in agreement with literature on lactoperoxidase, of which the Raman spectra closely resemble those of EPO (Manthey et al., 1986: 413.1 nm excitation, see also footnote 1). Instead, in Sibbett's work these bands were assigned to the non-totally symmetric modes ν_{11} (B_{1g}) and ν_{28} (B_{2g}). However, these bands would not be expected to be enhanced with Soret excitation. The large difference between the depolarization ratio of the 1561 cm^{-1} band upon Soret excitation ($\rho = 0.2$) and the band at 1558 cm^{-1} found upon Q_v-band excitation ($\rho = 0.8$) is most likely due to the spectral overlap between the polarized ν_2 (A_{1g}) and anomalously polarized ν_{19} (A_{2g}) vibrational modes. Because in Sibbett's work ν_2 and ν_3 were assigned to the bands at 1581 and 1512 cm^{-1} (1520 cm^{-1} in our spectra), the assignment of these lines was also revised. They are now assigned to ν_{37} and ν_{38} in accordance with the assignments for lactoperoxidase (Manthey et al., 1986) and horseradish peroxidase (Smulevich et al., 1991a). Raman activity is induced into these infrared (E_u under D_{4h} symmetry) vibrational modes via loss of the symmetry center of the heme prosthetic group due to the asymmetric conjugation of vinyl peripheral substituents. Other E_u vibrational modes are found at 1120 cm^{-1} (ν_{44}), 989 cm^{-1} (ν_{45}), and 275 cm^{-1} (ν_{52}; tentative assignment, the totally symmetric mode ν_9 is also expected in this spectral region (Choi et al., 1982a, b; Manthey et al., 1986). Vinyl modes, in turn, are enhanced through their coupling to in-plane porphyrin skeletal vibrations (Choi et al, 1982a) and are found at 1307, 1340, 1424, and ~1616 cm^{-1} (overlapping with ν_{10}) in the high wave-

number region and at 337 and 410 cm^{-1} in the low wavenumber region (see Table 1 and below).

The depolarized band at 1547 cm^{-1} is strongly resonance-enhanced upon excitation in the CT-band (Figs. 2 and 3) and is present as a weak low frequency shoulder of the ν_2/ν_{19} band in Fig. 4 (Q_v-excitation) and is assigned to ν_{11} (B_{1g}).

The intense polarized band at 1004 cm^{-1}, accompanied by weak bands at 1032 and 622 cm^{-1}, is typical for phenylalanine (Tu, 1982)

In the wavenumber region below 700 cm^{-1}, polarized bands are present in the Soret-and CT-excitation Raman spectra (Figs. 2, 3, 6, and 7). No intense depolarized or anomalously polarized bands are detected in accordance with the absence of low cm^{-1} bands in the Q_v-Raman spectra (Fig. 5). The EPO low wavenumber spectrum bears great resemblance to those of hog mucosa intestinal peroxidase (Kimura et al., 1981) lactoperoxidase (Manthey et al., 1986) and myeloperoxidase (Fig. 7).

In accordance with Choi and Spiro (1983), the lines around 500 cm^{-1} are assigned to pyrrole folding modes. A very strong line is found in the spectra obtained with Soret excitation (Figs. 6 and 7) at 410 cm^{-1}. Following the analysis of Manthey et al. (1986) for LPO, this line is assigned to the $\delta(C_bC_aC_\beta)$ (1) in-phase vinyl bending modes (Choi et al., 1982a, b). In this spectral region, some signal contributions may also be expected from a combination mode $\nu_{34} + \nu_{35}$ (Kitagawa et al., 1978; Kuila et al., 1985; Hildebrandt, 1990) and from iron-ligand stretching vibrations (e.g., Desbois et al., 1979). A contribution from such a mode cannot be excluded here. The peculiar excitation profile of the 408-cm^{-1} band in the CT-region (Fig. 4), different from the heme-macrocycle modes at 757, 1547, and 1614 cm^{-1}, is similar to that of the iron-ligand mode in MetHb-F (Asher et al., 1977).

Fig. 7 A, the low wavenumber Raman spectrum of EPO obtained with excitation in the Soret band, shows that the band at about 330 cm^{-1} is composed of two (or more) overlapping lines at 337 and 323 cm^{-1}. We assign the stronger component at 337 cm^{-1} to the $\delta(C_bC_aC_\beta)$ (2) out-of-phase vinyl bending mode analogous to the assignment made for lactoperoxidase (Manthey et al., 1986). The low frequency component is tentatively assigned to the porphyrin skeletal ν_8-mode (A_{1g}) (Choi et al., 1982a, b; Choi and Spiro, 1983), although it is clear that signal contributions in this spectral region may also be expected from other modes, such as, for example, the out-of-plane pyrrole tilting mode γ_6, which is activated in ruffled hemes (Czernuszewicz et al., 1989). Determination of the precise composition of the band at 330 cm^{-1} will require further experiments. In any case, the frequency of the ν_8-mode in EPO is apparently low in comparison with that of other protoheme proteins and complexes (Smulevich et al., 1991b; Choi and Spiro, 1983), where it is typically found at about 345 cm^{-1}.

The low wavenumber Raman spectra of plant peroxidases and many other protoheme proteins (Teraoka and Kitagawa, 1981; Choi and Spiro, 1983; Smulevich, 1993; Rousseau and Friedman, 1988; Sharma et al., 1989) show prominent bands

in the spectral interval from 350 to 380 cm^{-1}. These have been assigned to the overtone mode $2\nu_{35}$, in Fermi resonance with the ν_8-mode at about 345 cm^{-1} (Choi et al., 1982a; Choi and Spiro, 1983) and to a propionate bending mode at about 380 cm^{-1} (Hu and Spiro, 1994, unpublished data). In the EPO-spectra (and in the spectra of lactoperoxidase (Manthey et al., 1986), intestinal peroxidase (Kimura et al., 1981), and myeloperoxidase) lines are almost completely absent in this spectral interval (Fig. 7).

The $\sim$257-cm^{-1} band, enhanced with Soret excitation, is most likely due to the Fe-proximal His(N_ε) stretching mode. An analogous assignment was made in the case of lactoperoxidase (Manthey, 1986), although a definitive identification of this mode on the basis of ^{54}Fe isotope substitution experiments has only been accomplished for ferrous horseradish peroxidase (Teraoka and Kitagawa, 1981).

Structure of the prosthetic group

Oxidation state, spin state, Fe-coordination, and core size

From the positions of the modes in the high frequency region, information may be obtained concerning oxidation and spin state of the central iron and its coordination number. The frequency of the ν_4 band (1369 cm^{-1}) is at the low frequency side of the range for ferric hemeproteins ($\sim$1355–1362 cm^{-1} for ferrous, $\sim$1370–1376 cm^{-1} for ferric heme (Kitagawa, 1986; Mino et al., 1988)). The positions of the ν_3 (1485 cm^{-1}), ν_{11} (1547 cm^{-1}), ν_{19} (1558 cm^{-1}) and ν_{10} (1616 cm^{-1}) modes are characteristic for ferric high spin heme complexes (Sharma et al., 1989; Mino et al., 1988; Teraoka and Kitagawa, 1980).

The great similarity between absorption, EPR, and Raman spectra of EPO and lactoperoxidase suggests strongly that also in EPO the 5th ligand position is occupied by the nitrogen (N_ε) atom of histidine (Bolscher et al., 1984; Bolscher and Wever, 1984; Manthey et al., 1986). As mentioned, above the 257-cm^{-1} vibration is tentatively assigned to the Fe-His(N_ε) stretching mode. For peroxidases this mode is expected in the 240- to 260-cm^{-1} region, whereas for oxygen carriers, such as hemoglobin and myoglobin, it appears at $\sim$220 cm^{-1} (Teraoka, 1981). This difference is caused by the imidazolate character of the imidazole group as a result of a strong hydrogen bond between the histidine N_δ with a nearby amino acid side chain, which is a common feature of peroxidases (Kitagawa, 1988; Smulevich, 1993). The resonance enhancement of the Fe-His stretching mode indicates a significant out-of-plane displacement of the central iron. As was noted by Gilch et al. (1993), Raman spectra of planar hemes do not exhibit a ν(Fe-His) band. Stavrov (1993) showed that intensity and frequency of the ν(Fe-His) mode strongly depend on the Fe-out-of-plane distance.

The possibility of cysteine-sulfur at the 5th ligand position, whose strong π-electron donor capability would offer an explanation for the low frequency of the ν_4 mode of EPO, can be ruled out because of the absence of the characteristic Fe-S stretching mode at $\sim$350 cm^{-1} (Champion, 1988).

The positions of the ν_3 and ν_{10} bands do not enable a conclusive determination of the coordination number of the central iron. They are found in between the spectral regions characteristic for 6-coordinated (1478–1482 and 1605–1612 cm^{-1} for ν_3 and ν_{10}, respectively) and 5-coordinated (1487–1494 and 1622–1626 cm^{-1}) ferric high spin complexes (Sharma et al., 1989). Only the ν_{19} mode is found at a position characteristic for 6-coordinated high spin ferric heme complexes (Sharma et al., 1989; Mino et al., 1988). In spectra of native lactoperoxidase, ν_3 is also found at 1485 cm^{-1} but shifts down to 1478 cm^{-1} in the fluoride high spin complex (Manthey et al., 1986), whereas the ν_{10}-mode at 1616 cm^{-1} does not shift. For lactoperoxidase a weak 6th ligand is assumed, most likely H_2O, at 2.16 Å from the central iron (Kitagawa et al., 1983; Chang et al. 1993). The positions of the ν_3, ν_4, ν_{10}, and ν_{19} modes of EPO are very close to those of lactoperoxidase, aquomethmyoglobin, and aquomethemoglobin (Manthey et al., 1986; Mino et al., 1988), so a weakly bound H_2O-molecule at the 6th ligand position in EPO appears to be likely.

Both vinyl in-phase and out-of-phase modes, characteristic for a protoporphyrin IX heme, are detected (scissoring modes at $\sim$1424 and 1340 cm^{-1}, porphyrin-vinyl stretching modes at 1177 and 1120 cm^{-1}, and vinyl bending modes at 410 and 337 cm^{-1} (Choi et al., 1983)).

The existence of a ferric, high spin, 6-coordinated protoporphyrin IX as the active site for the EPO in the (unactivated) cells is in agreement with the EPR literature on eosinophils (Wever et al., 1980) and isolated EPO (Bolscher et al., 1983; 1984), and with Raman literature on isolated EPO (Sibbett et al., 1985).

It has been proposed that lactoperoxidase and myeloperoxidase have a prosthetic group in which a peripheral methyl group of protoporphyrin IX is replaced by a mercaptomethylene group (Nichol et al., 1987; Thanabal and La Mar, 1989; Dugad et al., 1990). The Raman spectra of the enzymes do not provide information about this matter, because no enhancement of the modes of this peripheral group or the methyl groups similar to the enhancement of the vinyl modes occurs.

Based on the empirical relationships, reported by Parthasarathi et al. (1987), between the frequencies of the metalloporphyrin vibrational modes in the high wavenumber region and porphyrin core size, the distance from the center of the porphyrin plane to the pyrrole nitrogens in EPO was determined to be $\sim$2.04 Å (largest value found was 2.053 Å for ν_{19}; lowest value 2.025 Å for ν_3), equal to that of lactoperoxidase (Chang et al., 1993) and close to that of intestinal peroxidase (2.05 Å: Kimura et al., 1981).

Heme-protein interactions

As noted above, the low wavenumber region of EPO is quite unusual. The in-phase and out-of-phase in-plane vinyl bending modes at 410 and 337 cm^{-1} are very strong (Figs. 6 and 7). These lines are also very strong in spectra of pig intestinal peroxidase (Kimura et al., 1981), lactoperoxidase (Manthey

et al., 1986), and myeloperoxidase (Babcock et al., 1985), but absent or much less prominent in spectra of other protoporphyrin-IX proteins such as (leg)hemoglobin (Rousseau et al., 1983), myoglobin, horseradish peroxidase (Kitagawa et al., 1983), ferrous manganese peroxidase (Mino et al., 1988), chloroperoxidase (Bangcharoenpaurpong et al., 1986), and bovine liver ferric catalase (Chuang et al., 1989).

A possible explanation could be that the orientation of the vinyl groups with respect to the porphyrin plane, constrained by the protein, in these mammalian peroxidases is different from that in other protoheme proteins, enabling a stronger conjugation to the porphyrin π-electron system. It has been proposed that the orientation of the vinyl substituents influences their electron-withdrawing ability, providing a mechanism for controlling the reduction potential (Reid et al., 1986), or that it may play a role in determining ligand binding affinity of hemes (Rousseau et al., 1983).

Also, the relatively low frequency of the ν_8-mode, which is a coupled Fe-pyrrole breathing and pyrrole-peripheral substituent bending mode and which was found to depend on the orientation of the peripheral (ethyl-)groups in nickel octaethylporphyrin (Li et al., 1989, 1990), may be indicative of differences in orientation of the vinyls (and other peripheral substituents) between the mammalian peroxidases and other protoheme proteins. The low frequency of the ν_8-mode moreover provides a possible explanation for the absence of the $2\nu_{35}$ band, because a larger frequency difference between the modes will decrease Fermi-resonance interaction.

The absence of a propionate bending mode around 380 cm^{-1} (Hu and Spiro, 1994, unpublished data) is another remarkable feature. It may be due to a specific propionate-protein interaction. A recent x-ray crystal study of myeloperoxidase has indicated that one of the heme propionates of that enzyme might participate in ionic interactions with nearby arginine residues (333 and 424), whereas the other is within hydrogen bonding distance of the side-chain hydroxyl of threonine 329 (Zeng and Fenna, 1992).

The low wavenumber Raman spectra of Fig. 7 support the notion of a distinct class of mammalian peroxidases with a characteristic set of heme-protein interactions, which includes lactoperoxidase, intestinal peroxidase, EPO, and perhaps also myeloperoxidase. This would be in agreement with observations reported in the literature. A family of homologous peroxidases was proposed by Ten et al. (1989) and by Zeng and Fenna (1992), based on the fact that the amino acid sequence of lactoperoxidase, myeloperoxidase, and EPO is highly conserved, especially in the immediate environment of the heme. Bolscher et al. (1984) concluded that the haem crevices of EPO and lactoperoxidase are very similar, on the basis of results obtained by absorption spectroscopy and EPR. Dugad et al. (1990) found that the ^{1}H NMR spectra of the cyanide-ligated complexes of bovine lactoperoxidase and myeloperoxidase are strikingly similar, and concluded that the prosthetic groups of these enzymes as well as their linkage to the protein matrix are likely to be very similar.

Comparison of EPO and lactoperoxidase

The largest differences between the Soret spectra of EPO in situ and those of lactoperoxidase (Manthey et al., 1986) are the frequencies of the ν_2, ν_{37}, and vinyl $\nu(C{=}C)$ vibrational modes.

The ν_2 and ν_{37} modes are strongly coupled to the vinyl $\nu(C{=}C)$ mode. This coupling might be influenced by the orientations of the vinyl groups, fixed by the protein, affecting the frequencies of all three modes (Choi et al., 1982b; Smulevich, 1993; Hashimoto, 1986).

In nickel protoporphyrin the ν_2 mode is downshifted by 9 cm^{-1} and the ν_{37} mode upshifted by 6 cm^{-1} with respect to the frequencies of these modes in nickel octaethylporphyrin due to coupling with the vinyl stretching vibration. In contrast with this no wavenumber shifts were noted for the ν_3, ν_{19} and ν_{10} modes, indicating the absence of kinematic coupling of these modes with vinyl modes (Choi et al., 1982a; 1982b). This resembles the differences between EPO and lactoperoxidase, where the ν_2 and ν_{37} frequencies are 7 cm^{-1} higher and 7 cm^{-1} lower respectively in EPO than in lactoperoxidase, but where the ν_3, ν_{19} and ν_{10} modes are found at the same frequencies (Manthey et al., 1986) implying a stronger coupling between heme skeletal modes and vinyl modes in lactoperoxidase than in EPO.

CONCLUSION

We have demonstrated that EPO can be structurally characterized in vivo by combining Raman data obtained at different excitation wavelengths and determining depolarization ratios of the Raman bands. From the assignments of the Raman bands, which partly revise and supplement previous assignments made for the isolated enzyme, we conclude that the active site of the EPO in the unactivated cell is a ferric, high spin, 6-coordinated, protoporphyrin IX, in agreement with literature on the isolated EPO. The pyrrole-nitrogen Fe distance was determined to be 2.04 Å, and the presence of the Fe-His(N$_\epsilon$) stretching mode in the spectra indicates that the central iron is displaced from the porphyrin plane. The proximal histidine was found to have the imidazolate character, characteristic for peroxidases, due to a strong hydrogen bond between the His(N$_\delta$) and a nearby amino acid residue.

Their unusual low wavenumber Raman spectrum suggests that mammalian peroxidases, including EPO, lactoperoxidase, intestinal peroxidase, and myeloperoxidase, differ from other protoheme proteins in the orientation of the peripheral vinyl groups and in interactions between heme-propionates and protein. High resolution x-ray studies of crystals of these peroxidases and Raman experiments with model compounds are needed to shed further light on this matter.

The possibilities for Raman experiments with single whole cells, in general, have been addressed recently (Greve and Puppels, 1993). Optimum conditions, i.e., laser wavelength, laser power, and signal integration times, which will minimize or prevent autofluorescence and prevent photodegradation of the molecules of interest have to be determined for each specific experiment. Minimum detectable concentra-

tions also depend strongly on the specific type of molecule studied and on the "background" Raman signal generated by other molecules present. With a measuring volume of approximately 1 μm^3 (10^{-15} ml), as was used in the present study, DNA in a concentration ≥ 10 mM and carotenoids in a concentration ≥ 10 μM are readily detectable. Spectra of chromatin have been obtained from the nucleus of single cells and of myeloperoxidase (estimated concentration 50–100 μM) from granules in the cytoplasm of human neutrophilic granulocytes (Puppels et al., 1991b), and the subcellular distribution of carotenoids in human lymphocytes has been determined (Puppels et al., 1993) under experimental conditions similar to those employed here.

The possibility of obtaining Raman spectra of peroxidases in single living cells, as was demonstrated here, not only enables a comparison of data obtained in vitro and in situ but, moreover, should enable investigations in which changes in enzyme active site structure and ligands, resulting from processes taking place in a cell, are determined and monitored.

REFERENCES

Abe, M., T. Kitagawa, and Y. Kyogoku. 1978. Resonance Raman spectra of octaethylporphyrinato-Ni(II) and meso-deuterated and ^{15}N substituted derivatives. II. A normal coordinate analysis. *J. Chem. Phys.* 69: 4526–4534.

Asher, S. A., L. E. Vickery, T. M. Shuster, and K. Sauer. 1977. Resonance Raman spectra of Methemoglobin derivatives. Selective enhancement of axial ligand vibrations and lack of an effect of inositol hexaphosphate. *Biochemistry.* 16:5849–5856.

Babcock, G. T., R. T. Ingle, W. A. Oertling, J. C. Davis, B. A. Averill, C. L. Hulse, D. J. Stufkens, B. G. J. M. Bolscher, and R. Wever. 1985. Raman characterization of human leukocyte myeloperoxidase and bovine spleen green haemoprotein. Insight into the chromophore structure and evidence that chromophores of myeloperoxidase are equivalent. *Biochim. Biophys. Acta.* 828:58–66.

Bakkenist, A. R. J., R. Wever, I. Vulsma, H. Plat, and B. F. van Gelder. 1978. Isolation procedure and some properties of myeloperoxidase from human leukocytes. *Biochim. Biophys. Acta.* 524:45–54.

Barnes, D., S. Aggarwal, S. Thomsen, M. Fitzmaurice, and R. Richards-Kortum. 1993. A characterization of the fluorescent properties of circulating human eosinophils. *Photochem. Photobiol.* 58:297–303.

Bolscher, B. G. J. M., H. Plat, and R. Wever. 1983. Some properties of human eosinophil peroxidase, a comparison with other peroxidases. *Biochim. Biophys. Acta.* 784:177–186.

Bolscher, B. G. J. M., and R. Wever. 1984. The nitrosyl compounds of ferrous animal peroxidases. *Biochim. Biophys. Acta.* 791:75–81.

Bremard, C., P. Dhamelincourt, J. Laureyns, and G. Turrel. 1985. The effect of high-numerical-aperture objectives on polarization measurements in micro-Raman spectrometry. *Appl. Spectrosc.* 39:1036–1039.

Butterfield, J. H., D. E. Maddox, and G. J. Gleich. 1984. The eosinophil

leukocyte: maturation and function. *Clin. Immunol. Rev.* 2:187–306.

Champion, P. M. 1988. Cytochrome P450 and the transform analysis of heme protein Raman spectra. *In* Biological Applications of Raman Spectroscopy. Vol. 3. T. G. Spiro, editor. Wiley & Sons, New York. 249–292.

Chang, C.-S., R. Sinclair, S. Khalid, I. Yamazaki, S. Nakamura, and L. Powers. 1993. An extended X-ray absorption fine structure investigation of the structure of the active site of lactoperoxidase. *Biochemistry.* 32: 2780–2786.

Choi, S., J. J. Lee, Y. H. Wei, and T. G. Spiro. 1983. Resonance Raman and electronic spectra of heme a complexes and cytochrome oxidase. *J. Am. Chem. Soc.* 105:3692–3707.

Choi, S., and T. G. Spiro. 1983. Out-of-plane deformation modes in the resonance Raman spectra of metalloporphyrins and heme proteins. *J. Am. Chem. Soc.* 105:3683–3692.

Choi, S., T. G. Spiro, K. C. Langry, and K. M. Smith. 1982a. Vinyl influences on protoheme resonance Raman spectra: Nickel(II) protoporphyrin IX with deuterated vinyl groups. *J. Am. Chem. Soc.* 104:4337–4344.

Choi, S., T. G. Spiro, K. C. Langry, K. M. Smith, D. L. Budd, and G. N. La Mar. 1982b. Structural correlations and vinyl influences in resonance Raman spectra of protoheme complexes and proteins. *J. Am. Chem. Soc.* 104:4345–4351.

Chuang, W. J., J. Heldt, and H. E. Van Wart. 1989. Resonance Raman spectra of bovine liver catalase compound II. *J. Biol. Chem.* 264: 14209–14215.

Czernuszewicz, R. S., X.-Y. Li, and T. G. Spiro. 1989. Nickel octaethylporphyrin ruffling dynamics from resonance Raman spectroscopy. *J. Am. Chem. Soc.* 111:7024–7031.

De Mul, F. F. M., and J. Greve. 1993. RAMPAC: a program for analysis of complicated Raman spectra. *J. Raman Spectrosc.* 24:245–250.

Desbois, A., M. Lutz, and R. Banerjee. 1979. Low-frequency vibrations in resonance Raman spectra of horse heart myoglobin. Iron-ligand and iron-nitrogen vibrational modes. *Biochemistry.* 18:1510–1518.

Dugad, L. B., G. N. La Mar, H. C. Lee, M. Ikeda-Saito, K. S. Booth, and W. S. Caughey. 1990. A nuclear Overhauser effect study of the active site of myeloperoxidase. Structural similarity of the prosthetic group to that of lactoperoxidase. 1990. *J. Biol. Chem.* 265:1737–7179.

Eaton, W. A., and R. M. Hochstrasser. 1968. Single-crystal spectra of ferrimyoglobin complexes in polarized light. *J. Chem. Phys.* 49:985–995.

Fuerst, D. E., and J. R. Jannach. 1965. Autofluorescence of eosinophils: a bone marrow study. *Nature.* 205:1333–1334.

Gilch, H., R. Schweitzer-Stenner, and W. Dreybrodt. 1993. Structural heterogeneity of teh Fe^{2+}-N_ϵ(His^{F8}) bond in various hemoglobin and myoglobin derivatives probed by the Raman-active iron histidine stretching mode. *Biophys. J.* 65:1470–1485.

Gleich, G. J., and C. R. Adophson. 1986. The eosinophil leukocyte: structure and function. *In* Advances in Immunology. Vol. 39. F. J. Dixon, editor. Academic Press, Orlando, FL. 177–253.

Greve, J., and G. J. Puppels. 1993. Raman microspectroscopy of single whole cells. *In* Biomolecular Spectroscopy, Part A. R. J. H. Clark and R. E. Hester, editors. Wiley & Sons, Chichester. 231–265.

Grooth, B. G. de, L. W. M. M. Terstappen, G. J. Puppels, and J. Greve. 1987. Light-scattering polarization measurements as a new parameter in flow cytometry. *Cytometry.* 8:539–544.

Kimura, S., I. Yamazaki, and T. Kitagawa. 1981. Unusual low-frequency resonance raman spectra of heme observed for hog intestinal peroxidase and its derivatives. *J. Am. Chem. Soc.* 20:4632–4638.

Kitagawa, T. 1986. Resonance Raman spectra of reaction intermediates of heme enzymes. *In* Spectroscopy of Biological Systems. R. J. H. Clark and R. E. Hester, editors. Wiley & Sons, Chichester. 443–481.

Kitagawa, T. 1988. The heme protein structure and the iron histidine stretching mode. In "Biological applications of Raman spectroscopy" vol. 3 (Spiro, T. G., editor). John Wiley & Sons, New York, 97–131.

Kitagawa, T., M. Abe, and H. Ogoshi. 1978. Resonance Raman spectra of octaethylporphyrinato-Ni (II) and meso-deuterated and ^{15}N-substituted derivatives. I. Observation and assignments of nonfundamental Raman lines. *J. Chem. Phys.* 69:4516–4525.

Kitagawa, T., S. Hashimoto, J. Teraoka, N. Shingo, H. Yajima, and T. Hosoya. 1983. Distinct heme-substrate interactions of lactoperoxidase probed by resonance Raman spectroscopy: difference between animal and

plant peroxidases. *Biochemistry.* 22:2788–2792.

Klebanoff, S. J., J. M. Agosti, A. Jorg, and A. M. Waltersdorph. 1989. Comparative toxicity of the horse eosinophil peroxidase-H_2O_2-halide system and granule basic proteins. *J. Immunol.* 143:239–244.

Klebanoff, S. J., and R. A. Clark. 1978. The Neutrophil: Function and Clinical Disorders. North-Holland, Amsterdam.

Koenderman, L., P. T. M. Kok, M. L. Hamelink, A. J. Verhoeven, and P. L. B. Bruijnzeel. 1988. An improved method for the isolation of eosinophilic granulocytes from peripheral blood of normal individuals. *J. Leukocyte Biol.* 44:79–86.

Li, X.-Y., R. S. Cscznuszewicz, J. R. Kincaid, and T. G. Spiro. 1989. Consistent porphyrin force field. 3. Out-of-plane modes in the Resonance Raman spectra of plants and ruffled nickel octaethylporphyin. *J. Am. Chem. Soc.* 111:7012–7023.

Li, X.-Y., R. S. Csernuszewicz, J. R. Kincaid, P. Stein, and T. G. Spiro. 1990. Consistent porphyrin force field. 2. Nickel Octaethylporphyrin skeletal and substituent mode assignments from ^{15}N, meso-d_4, and methylene-d_{16} Raman and infrared isotope shifts. *J. Phys. Chem.* 94:47–61.

Manthey, J. A., N. J. Boldt, D. F. Bocian, and S. I. Chan. 1986. Resonance Raman studies of lactoperoxidase. *J. Biol. Chem.* 261:6734–6741

Mino, Y., H. Wariishi, N. J. Blackburn, T. M. Loehr, and M. H. Gold. 1988. Spectral characterization of manganese peroxidase, an extracellular heme enzyme from the lignin-degrading Basidiomycete, Phanerochaete chrysosporium. *J. Biol. Chem.* 263:7029–7036.

Nichol, A. W., L. A. Angel, T. Moon, and P. S. Clezy. 1987. Lactoperoxidase haem, an iron-porphyrin thiol. *Biochem. J.* 247:147–150.

Parker, C. W. 1984. Effector mechanisms of immunity. Mediators: release and function. *In* Fundamental Immunology. W. E. Paul, editor. Raven Press, New York. 697–747.

Parthasarathi, N., C. Hansen, S. Yamaguchi, and T. G. Spiro. 1987. Metalloporphyrin core size resonance Raman marker bands revisited: implications for the interpretation of hemoglobin photoproduct Raman frequencies. *J. Am. Chem. Soc.* 109:3865–3871.

Puppels, G. J., W. Colier, J. H. F. Olminkhof, C. Otto, F. F. M. De Mul, and J. Greve. 1991a. Description and performance of a highly sensitive confocal Raman microspectrometer. *J. Raman Spectrosc.* 22:217–225.

Puppels, G. J., F. F. M. De Mul, C. Otto, J. Greve, M. Robert-Nicoud, D. J. Arndt-Jovin, and T. M. Jovin. 1990. Studying single living cells and chromosomes by confocal Raman microspectroscopy. *Nature.* 347:301–303.

Puppels, G. J., H. S. P. Garritsen, J. A. Kummer, and J. Greve. 1993. Carotenoids located in human lymphocyte subpopulations and natural killer cells by Raman microspectroscopy. *Cytometry.* 14:251–256.

Puppels, G. J., H. S. P. Garritsen, G. M. J. Segers-Nolten, F. F. M. De Mul, and J. Greve. 1991b. Raman microspectroscopic approach to the study of human granulocytes. *Biophys. J.* 60:1046–1056.

Ramsey, P. G., T. Martin, E. Chi, and S. J. Klebanoff. 1982. Arming of mononuclear phagocytes by eosinophil peroxidase bound to staphylococcus aureus. *J. Immunol.* 128:415–420.

Reid, L. S., A. R. Lim, and A. G. Mauk. 1986. Role of heme vinyl groups in cytochrome b5 electron transfer. *J. Am. Chem. Soc.* 108:8197–8201.

Rousseau, D. L., M. R. Ondrias, G. N. LaMar, S. B. Kong, and K. M. Smith. 1983. Resonance Raman spectra of the heme in leghemoglobin: evidence for the absence of ruffling and the influence of vinyl groups. *J. Biol. Chem.* 258:1740–1746.

Rousseau, D. L., and J. M. Friedman. 1988. Transient and cryogenic studies of photodissociated hemoglobin and myoglobin. *In* Biological Applications of Raman Spectroscopy. Vol. 3 (T. G. Spiro, editor). Wiley & Sons, New York. 133–215.

Samoszuk, M. K., and F. P. Espinoza. 1987. Deposition of autofluorescent granules in pathologic bone marrow biopsies. *Blood.* 70:597–599.

Sharma, K. D., L. A. Andersson, T. M. Loehr, J. Terner, and H. M. Goff. 1989. Comparative spectral analysis of mammalian, fungal and bacterial catalases. *J. Biol. Chem.* 264:12772–12779.

Sibbett, S. S., S. J. Klebanoff, and J. K. Hurst. 1985. Resonance Raman characterization of the heme prosthetic group in eosinophil peroxidase. *FEBS Lett.* 189:271–275.

Smulevich, G. 1993. Structure-function relationships in peroxidases via resonance Raman spectroscopy and site-directed mutagenesis: cytochrome c peroxidase. *In* Biomolecular Spectroscopy Part A. R. J. H. Clark and R. E. Hester, editors. Wiley & Sons, Chichester. 163–193.

Smulevich, G., A. M. English, A. R. Mantini, and M. P. Marzocchi. 1991a. Resonance Raman investigation of ferric iron in horseradish peroxidase and its aromatic donor complexes at room and low temperatures. *Biochemistry.* 30:772–779.

Smulevich, G., M. A. Miller, J. Kraut, and T. G. Spiro. 1991b. Conformational change and histidine control of the heme chemistry in cytochrome c peroxidase: resonance Raman evidence from Leu-52 and Gly-181 mutants of cytochrome c peroxidase. *Biochemistry.* 30:9546–9558.

Spiro, T. G. 1975. Resonance Raman spectroscopic studies of heme proteins. *Biochim. Biophys. Acta.* 416:169–189.

Spiro, T. G., and X.-Y. Li. 1988. Resonance Raman spectroscopy of metalloporphyrins. *In* Biological Applications of Raman Spectroscopy. Vol. 3. Wiley & Sons, New York. 1–37.

Spiro, T. G., and T. C. Strekas. 1974. Resonance Raman spectra of heme proteins. Effects of oxidation and spin state. *J. Am. Chem. Soc.* 96:338–345.

Stavrov, S. S. 1993. The effect of iron displacement out of the porphyrin plane on the resonance Raman spectra of heme proteins and iron porphyrins. *Biophys. J.* 65:1942–1950.

Ten, R. M., L. R. Pease, D. J. McKean, M. P. Bell, and G. J. Gleich. 1989. Molecular cloning of the human eosinophil peroxidase. Evidence for the existence of a peroxidase multigene family. *J. Exp. Med.* 169:1757–1769.

Tepper, R. I., R. L. Coffman, and P. Leder. 1992. An eosinophil-dependent mechanism for the anti tumor effect of interleukin 4. *Science.* 257:548–551.

Teraoka, J., and T. Kitagawa. 1980. Raman characterization of axial ligands for penta- and hexacoordinate ferric high- and intermediate-spin (octaethylporphyrinato) iron(III) complexes. Elucidation of unusual resonance Raman spectra of cytochrome c. *J. Phys. Chem.* 84:1928–1935.

Teraoka, J., and T. Kitagawa. 1981. Structural implication of the heme-linked ionization of horseradish peroxidase probed by the Fe-histidine stretching Raman line. *J. Biol. Chem.* 256:3969–3977.

Teraoka, J., T. Ogura, and T. Kitagawa. 1982. Resonance Raman spectra of the reaction intermediates of horseradish peroxidase catalysis. *J. Am. Chem. Soc.* 104:7354–7356.

Terner, J., and D. E. Reed. 1984. Resonance Raman spectroscopic characterization of the heme coordination and spin state in the alkaline form of horseradish peroxidase. *Biochim. Biophys. Acta.* 789:80–86.

Thanabal, V., and G. N. La Mar. 1989. A nuclear Overhauser effect of the molecular and electronic structure of the heme crevice in lactoperoxidase. *Biochemistry.* 28:7038–7044.

Tu, A. T. 1982. Raman Spectroscopy in Biology: Principles and Applications. Wiley & Sons, New York.

Turrell, G. 1984. Analysis of polarization measurements in Raman spectroscopy. *J. Raman Spectrosc.* 15:103–108.

Weil, G. J., and T. M. Chused. 1981. Eosinophil autofluorescence and its use in isolation and analysis of human eosinophils using flow microfluorimetry. *Blood.* 57:1099–1104.

Wever, R., N. Hamers, R. S. Weening, and D. Roos. 1980. Characterization of the peroxidase in human eosinophils. *Eur. J. Biochem.* 108:491–495.

Wever, R., H. Plat, and M. N. Hamers. 1981. Human eosinophil peroxidase: a novel isolation procedure, spectral properties and chlorinating activity. *FEBS Lett.* 123:327–331.

Zeng, J., and R. E. Fenna. 1992. X-ray crystal structure of canine myeloperoxidase at 3 Å resolution. *J. Mol. Biol.* 226:185–207.